Supporting Information:

Characterization of the active form of pradimicin-S

Syed Shahzad-ul-Hussan,[†] Rodolfo Ghirlando,[‡] Cajetan I. Dogo-Isonagie,[†] Yasuhiro Igarashi,[§] Jan Balzarini,[||] Carole A. Bewley[†]*

[†]Laboratory of Bioorganic Chemistry and [‡]Laboratory of Molecular Biology, National Institute of Diabetes and Digestive and Kidney Diseases, National Institutes of Health, Bethesda, MD 20892
[§]Biotechnology Research Center, Toyama Prefectural University, Imizu, Toyama 939-0398, Japan
[||]Rega Institute for Medical Research, Katholieke Universiteit Leuven, Leuven, Belgium

General Experimental Methods

Analytical ultracentrifugation

Sedimentation velocity: Sedimentation velocity experiments were conducted at 20.0°C and 50,000 rpm on a Beckman Coulter ProteomeLab XL-I analytical ultracentrifuge. Samples of PRM-S were prepared at required concentrations in either 50 mM MOPS (pH 7.0), 0.5 mM EDTA or 50 mM MOPS (pH 7.0) containing 5 mM $CaCl_2$. One or two equivalents of mannobiose or mannotriose were included when required. All samples were loaded into 2-channel, 12 or 3 mm path length sector shaped cells and thermally equilibrated at zero speed. Velocity scans were subsequently acquired at approximately 7 min intervals in a continuous mode as single absorbance measurements at 280 nm using a radial spacing of 0.003 cm. Data were analyzed in SEDFIT 12.52[1] in terms of a continuous c(*s*) distribution using an *s* range of 0 to 2.5 (in the absence of calcium) or 5 (in the presence of calcium) with a linear resolution of 100 and a maximum entropy regularization confidence interval of 0.68. In all cases, excellent fits were observed with root mean square deviations ranging from 0.0025 – 0.0065 absorbance units. A partial specific volume of 0.622 $cm^3\,g^{-1}$ was calculated for PRM-S based on its chemical composition using the methods described by Durchschlag and Zipper.[2,3] Solution densities ρ were measured at 20.00°C on a Mettler Toledo DE51 density meter and solution viscosities η were measured at 20.00°C using an Anton Paar AMVn rolling ball viscometer. Sedimentation coefficients were corrected to standard conditions.

Sedimentation equilibrium: Sedimentation equilibrium experiments were conducted at 20.0°C on a Beckman Optima XL-A analytical ultracentrifuge. PRM-S solutions were studied at concentrations of 10 and 40 μM in 50 mM MOPS (pH = 7.0), 0.5 mM EDTA; and 10 μM PRM-S in 50 mM MOPS (pH = 7.0) containing 5 mM $CaCl_2$. Samples were loaded into 2-channel, 12 mm path length sector shaped cells (160 μL). Data were collected at 40,000, 50,000 and 60,000 rpm at 280 nm as an average of 4 absorbance measurements using a radial spacing of 0.001 cm. Sedimentation equilibrium at each speed was achieved within 55 h. Data were analyzed globally using SEDPHAT 9.4[4] in terms of non-interacting species models.

NMR Spectroscopy

NMR data were recorded on 500 or 600 MHz spectrometers equipped with *z*-shielded gradient cryoprobes, and a sample temperature of 298K. PRM-S and PRM-A solutions were prepared by dissolving lyophilized powder in 99.9% D_2O to give desired concentrations. The pH of all solutions was adjusted to 7.0 using 0.1 M NaOH or HCl if necessary. STD NMR spectra were acquired as

described in detail previously,[5,6] with selective irradiation at 0.5 and 40 ppm for on and off resonance spectra, respectively, using a train of 50 ms Gaussian-shaped radio frequency pulses separated by 1 ms delays. Complexes used for STD NMR included PRM-S/Manα1-3(Manα1-6)Man, PRM-S/Manα1-2Man, PRM-S/*O*-methyl mannoside, and PRM-S/$GlcNAc_2$ with concentrations of 50 μM PRM-S to 800 μM carbohydrate ligand.

Surface Plasmon Resonance

SPR analyses were performed on a Biacore T100 instrument. In these experiments fully glycosylated gp120, strain ZM109, was immobilized on a CM5 sensor chip and kinetic analysis of PRM-S binding to gp120 was performed by injecting PRM-S at varying concentrations (2, 4, 8, 16, 32, 64 and 128 μM) onto the gp120-coated and reference surfaces at a flow rate of 60 µL/min for 60 s during the association phase. Subsequent to this step running buffer was injected at the same flow rate for 5 min constituting the dissociation phase. All binding data were obtained from two independent experiments (separate flow cells) and each analysis was performed in duplicate. Data were analyzed using the BIAevaluation software package.

To obtain high quality binding data, two separate sets of experiments were carried out. In the first, we calculated the amount of gp120 to be immobilized to give a desired response of ~100 response units (RUs) upon PRM-S binding according to the equation $R_L=(R_{max} \times mwt_L)\ (n \times mwt_A)^{-1}$, where R_{max} corresponds to the RUs at the highest analyte concentration used, R_L corresponds to the RUs as a function of the amount of ligand immobilized on the surface, *n* is the binding stoichiometry, and Mwt (L) and Mwt (A) are the molecular masses of gp120 and *monomeric* PRM-S, respectively. In this first data set, we observed R_{max} values up to 17-fold higher than the expected values for PRM-S binding to gp120. These increased values are likely due to the presence of PRM-S tetramers (or oligomers at concentrations greater than 100 μM), to a stoichiometry of binding of PRM-S to gp120 that is greater than one owing to the presence of multiple glycosylation sites on gp120, or a combination of the two. To obtain reliable kinetic data, we reduced the level of immobilized gp120 by approximately 15-fold, and performed a similar set of binding experiments using the same concentration series of PRM-S (data shown in Fig. 4a). This second data set gave excellent fits to a heterogeneous ligand model with K_D values of 2 and 32 μM (SI Table 2). In the absence of Ca^{2+}, we did not observe binding to gp120 at any of the concentrations tested (data not shown).

Env-pseudotyped HIV neutralization assays

Env-pseudotyped HIV neutralization assays were performed as described previously.[7] Serial dilutions of inhibitors were prepared and added to pseudotyped viral particles followed by freshly prepared TZM-bl indicator cells, a HeLa-derived cell line that has been genetically modified to constitutively express CD4, CCR5, and CXCR4. Plates were incubated at 37 °C overnight followed by addition of 150 µL fresh growth media. (D-MEM and E-MEM used for neutralization assays contain 0.5-1 mM Ca^{2+}.) Approximately 48 h post infection, cells were lysed and luciferase activity was measured using a BrightGlo luciferase assay kit (Promega, Madison, WI) in a Synergy2 luminescence microplate reader (BioTek Instruments, Inc., Winooski, VT). Pseudovirus stocks were diluted to yield a 200- to 1000-fold increase of luminescence over uninfected cells treated as background. Neutralizing activity was analyzed by non-linear least-squares fitting using the program Kaleidagraph 4.0 (Synergy Software, Reading, PA) and IC_{50} values were calculated using a simple dose-activity relationship $\%fusion=100/(1+[I]/IC_{50})$.

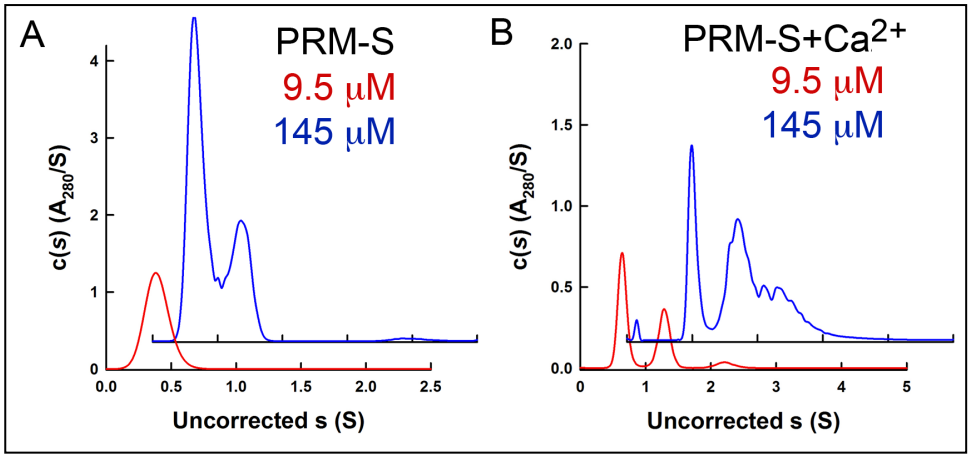

Figure S1. Analytical ultracentrifugation of solutions of PRM-S in the (A) absence and (B) presence of $CaCl_2$ at concentrations of 9.5 μM (in red) and 145 μM (in blue). In contrast to solutions of PRM-S at low micromolar concentrations (<10 μM), the presence of higher molecular weight species is evident at higher concentrations (>100 μM) in the presence and absence of $CaCl_2$. The more slowly sedimenting, major form of PRM-S in the presence of $CaCl_2$ (red curve, panel B) has a best-fit molar mass of 3350 ± 60 g mol^{-1}. This value corresponds to ~3.5 times the molecular weight of monomeric PRM-S, indicating an equilibrium between discrete oligomers.

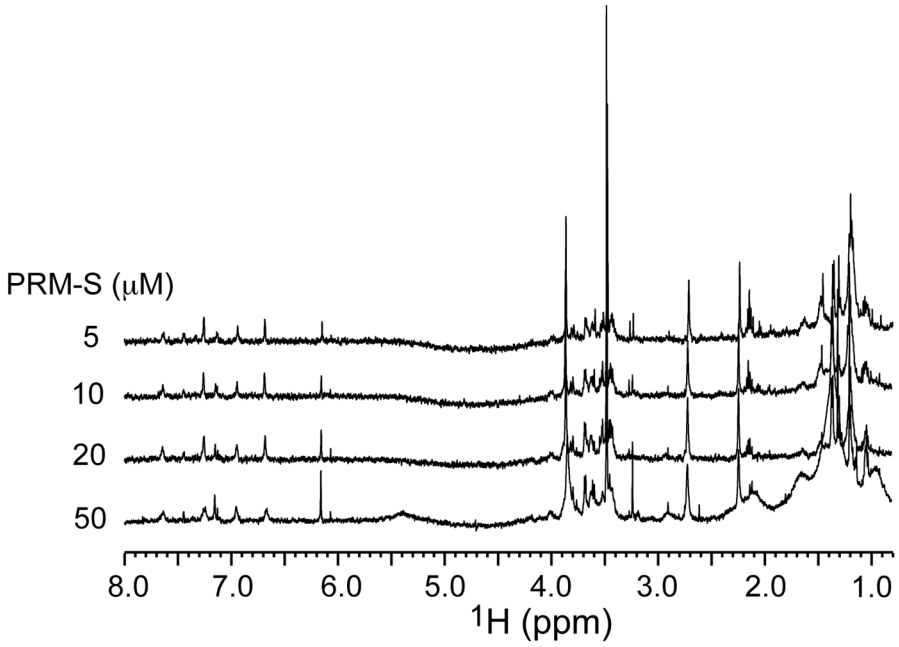

Figure S2. ^1H NMR spectra of increasing concentrations of PRM-S in the absence of $CaCl_2$. The spectra show that line broadening does not occur in the absence of Ca^{2+}, consistent with the analytical ultracentrifugation data that demonstrate PRM-S occurs as a monomer at low micromolar concentrations, and does not undergo self aggregation.

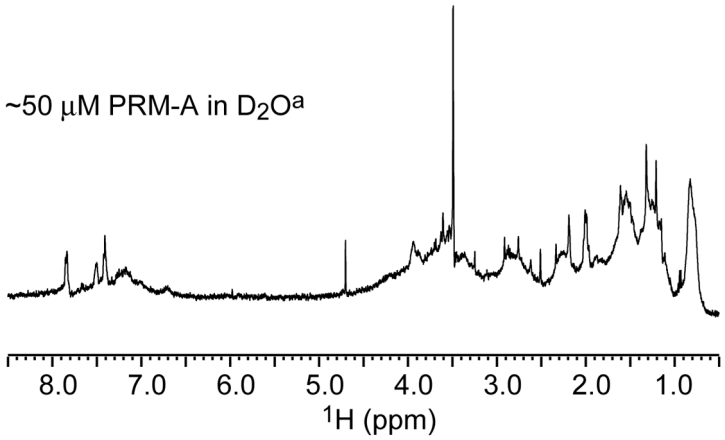

Figure S3. ^{1}H NMR spectrum of PRM-A (50 μM) in the *absence* of $CaCl_2$. In contrast to spectra of PRM-S recorded under identical conditions, the spectrum of PRM-A comprises only broadened, unresolved peaks indicative of aggregation. [a]Precipitation of solid aggregates was observed with all solutions of PRM-A; thus concentrations are estimated.

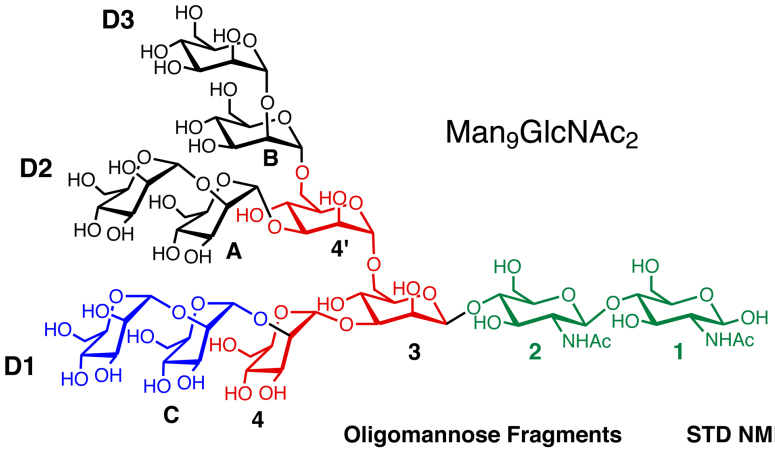

Oligomannose Fragments	STD NMR
Manα1-2Man	Weak
Manα1-3(Manα1-6)Man	Strong
$GlcNAc_2$	nb
Mannose	nb

Figure S4. Fragments of oligomannose used for ligand screening to PRM-S by STD NMR. Fragments are labeled in the table as shown in the chemical structure of $Man_9GlcNAc_2$.

Table S1. ^{1}H chemical shifts of mannotriose and mannobiose.[a]

	Mannotriose Manα1-3(Manα1-6)Man				**Mannobiose Manα(1-2)Man**	
Proton	Aα[b]	Aβ[b]	B[b]	C[b]	A[b]	B[b]
H-1	5.01	4.78	4.99	4.77	5.39	5.05
H-2	3.95	3.96	3.95	3.86	3.96	4.08
H-3	3.80	3.64	3.76	3.72	3.95	3.86
H-4	3.78	3.68	3.53	3.52	3.70	3.64
H-5	3.87	3.43	3.65	3.56	3.81	3.77
H-6a,b	3.54, 3.89	3.62, 3.846	3.63, 3.76	3.63, 3.76	3.76, 3.87	3.74, 3.89

[a]Spectra were recorded at 298 K, and samples prepared in 99.9% D_2O, pH 7.0.
[b]Pyranose rings are labeled as in Figure 3.

Table S2. Kinetics of PRM-S binding to HIV-1 gp120 as measured by surface Plasmon resonance.

Component	k_a (M^{-1} s^{-1})	k_d (s^{-1})	K_D (M)
1	$2.9 \times 10^3 \pm 28$	$9.4 \times 10^{-2} \pm 2.9 \times 10^{-4}$	3.2×10^{-5}
2	$3.9 \times 10^3 \pm 72$	$7.2 \times 10^{-3} \pm 2.0 \times 10^{-5}$	1.8×10^{-6}

References

1. Schuck, P. S. *Biophys. J.* **2000***, 78*, 1606.
2. Durchschlag, H.; Zipper, P. *Prog. Colloid Polym. Sci*. **1994***, 94*, 20.
3. Durchschlag, H.; Zipper, P. *J. Appl. Crystallogr*. **1997**, *30*, 803-807.
4. Schuck, P. *Anal. Biochem*. **2003** *320*, 104.
5. Mayer, M.; Meyer B. *J. Am. Chem. Soc.* **2001**, *123*, 610.
6. Lam, S. N.; Acharya, P.; Wyatt, R.; Kwong, P. D.; **Bewley, C. A.** *Bioorg. Med. Chem.* **2008**, *16*, 10113.
7. Li, M.; Gao, F.; Mascola, J. R.; Stamatatos, L.; Polonis, V. R.; Koutsoukos, M.; Voss, G.; Goepfert, P.; Gilbert, P.; Greene, K. M.; Bilska, M.; Kothe, D. L.; Salazar-Gonzalez, J. F.; Wei, X.; Decker, J. M.; Hahn, B. H.; Montefiori, D. C. *J. Virol.* **2005***, 79*, 10108.